보건학석사학위논문

Degradation kinetics and byproducts pathway of 1H-benzotriazole during UV/chlorination process

UV/Chlorination 공정 중 1H-benzotriazole의 분해 특성과 메커니즘에 관한 연구

2018 년 2 월

서울대학교 보건대학원

환경보건학과 환경보건학전공

이 정 은

Abstract

Degradation kinetics and byproducts pathway of 1H-benzotriazole during UV/chlorination process

Jung-Eun Lee

Department of Environmental Health Sciences

Graduate School of Public Health

Seoul National University

Benzotriazole (BTA) is widely used as a corrosion inhibitor of yellow metals, antifreezes, cutting fluids, and coating materials in various industries or even in domestic products. Because of its high polarity and low biodegradability, BTA is expected to be mobile in the aquatic environment. The reported removal of BTA

ranges between 29% and 58% in wastewater treatment plant. In this study, the removal kinetics and degradation mechanisms of BTA during UV/chlorination process were investigated, especially focusing on UV-A/chlorination process. The experiment was performed with batch type photo reactor. The light intensity of UV lamps (UV-A, B, C) used were 3.3 – 4.3 mW/cm^2. UHPLC- MS/MS was used for BTA analysis and UPLC-qTOF-MS was used for byproducts identification. The result showed that the removal rate of BTA was fast in the order of UV-C, UV-B, UV-A. UV-A/chlorination process showed a synergetic effect compared to UV-A photolysis and chlorination only processes. The synergetic effect is due to the OH radical generated in the UV/chlorination process. The kinetics followed the pseudo-first order kinetics. More chlorine dosage, faster removal rate was achieved. Alkaline pH increased the removal of BTA UV-A/chlorination process. Additionally, reaction byproducts during UV/chlorination process were identified (m/z 150.0307, 166.0252, 124.0147, 140.0071, 154.0245). Using the identified byproducts we proposed the degradation pathway of BTA during UV-A/chlorination process. Also, toxic profiles during UV-A/chlorination of BTA was investigated with Microtox bioassay. The ecotoxicity during UV-A/chlorination of BTA was decreased. As a result, it was confirmed that UV-A/Chlorination process was quite effective not only for BTA elimination, but also for ecotoxicity decrease.

Keywords: Benzotriazole, Non-biodegradable organic compounds, Advanced Oxidation Process, UV-A/chlorination, Degradation pathway

Student Number: 2016-24053

Contents

List of Figures

List of Tables

I. Introduction

1.1. Background

Recently, concerns about micropollutants that can adversely affect ecosystems and public health have been increasing. The development of analytical techniques has allowed us to monitor a variety of materials, but continuous monitoring of all substances is inefficient. Depending on how well known in the study are ecotoxicology, potential health effects, monitoring data, etc., it is necessary to select and manage substances for future regulatory purposes (Leonards & Lamoree).

1.2. Benzotriazole in water environment

1H-benzotriazole (BTA) has a characteristic to inhibit corrosion of yellow metal like copper, It is used for anti-corrosive agents in various industries, aircraft de-icer, and dishwashing detergents for protecting silver (Pillard, Cornell, DuFresne, & Hernandez, 2001). It is included in many domestic and industrial products. The annual production of BTA was 9000 t/year in USA (Hart, Davis, Erickson, & Callender, 2004; Liu, Ying, Shareef, & Kookana, 2011). It is expected to be in aquatic environment by the fact that it is a high polar compound (log Kow 1.44) (Reemtsma, Miehe, Duennbier, & Jekel, 2010).

The occurrence of BTA in water environment has been reported in several studies (Table 1). In surface water, BTA was detected at the concentration of several ppbs in

Germany, Switzerland, China and Spain, and several ppts in Korea. The highest concentration of 5.4 μg/L was in Switzerland. In WWTPs, 7.7, and 2.7 μg/L in effluents, and 12.0 and 6.6 μg/L in influent in Germany and China.

BTA in surface water might be originated from wastewater treatment plants (WWTPs). The removal efficiency of BTA in Conventional Activated Sludge (CAS) process was about only 37%, because it is not biodegradable well. In another process, 47% of BTA was eliminated in the combination process of activated sludge, stabilization lagoon and dissolved air flotation/filtration (Weiss, Jakobs, & Reemtsma, 2006), and 61% in membrane bioreactor process (Liu, Ying, Shareef, & Kookana, 2012). The residual BTA included in WWTP effluent, can be released to surface water.

Accordingly, in Switzerland, BTA was designated as one of the indicator pollutant that presents removal efficiency of WWTPs (Giannakis et al., 2015) (Table 2).

Table 1. Occurrence of 1H-benzotriazole in water environment.

Sample media	Conc. (μg/L)	Country	Reference
Surface water	0.9	Germany	(Weiss & Reemtsma, 2005)
Surface water	0.06-5.44	Switzerland	(Giger, Schaffner, & Kohler, 2006)
Surface water	0.639-3.69	Switzerland	(Voutsa, Hartmann, Schaffner, & Giger, 2006)
Surface water	ND-1.474	Germany	(Kiss & Fries, 2009)
Surface water	1.200-1.700	China	(Heeb et al., 2012)
Surface water	0.097-1.184	Spain	(Esteban et al., 2014)
Surface water	0.047-0.088	Korea	(Ryu, Oh, Snyder, & Yoon, 2014)
WWTP effluent	7.7±2.7	Germany	(Weiss et al., 2006)
WWTP effluent	2.671±0.278	China	(Liu et al., 2012)
WWTP influent	12.0±3.7	Germany	(Weiss et al., 2006)
WWTP influent	6.634±0.423	China	(Liu et al., 2012)

Table 2. The indicator pollutants in the Swiss legislation.(Giannakis et al., 2015)

Indicator type	List of 12 indicators (2016 enforcement)	Pollutant type
Very Well Eliminated	Amisulpride	Antidepressant
	Carbamazepine	Antiepileptic
	Citalopram	Antidepressant
	Clarithromycin	Antibiotic
	Diclofenac	Analgesic
	Hydrochlorothiazide	Diuretic
	Metoprolol	Beta blocker
	Venlafaxine	Antidepressant
Well Eliminated	Benzotriazole	Anticorrosive
	Candesartan	Angiotensin II Antagonist
	Irbesartan	Angiotensin II Antagonist
	Mecoprop	Herbicide

1.3. Toxicity of 1H-benzotriazole

Studies on the various toxicity of BTA have been increasing, but specific toxicity is still not found. The NOAEC (No Observed Adverse Effect Concentration, LOAEC (Lowest Observed Adverse Effect Concentration), and LC_{50} of BTA were 92, 184, and 120 mg/L for 48 hr for C.*dubia* (*Ceriodaphnia dubia*) (Pillard et al., 2001). In Freshwater alga growth inhibition test with *Desmodesmus subspicatus*, NOAEC and LOEC of it were 1.2, 2.5 mg/L, and there is no effect for reproduction test with *Daphnia magna* (Seeland, Oetken, Kiss, Fries, & Oehlmann, 2012). And it exhibited antiandrogenic activity in vitro study, but not in vivo (Fent, Chew, Li, & Gomez, 2014). Recently, studies on neurotoxicity and hepatotoxicity of BTA was studied (Duan et al., 2017; Liang, Martyniuk, Zha, & Wang, 2016; Liang, Zha, Martyniuk, Wang, & Zhao, 2017).

1.4. Advanced Oxidation Processes (AOPs)

Advanced oxidation processes are chemical treatments to mainly remove organic compounds in water treatment plants by oxidation through reactions with hydroxyl radicals which is one of the strongest oxidants (Glaze, Kang, & Chapin, 1987). The main parts of AOPs are formation of hydroxyl radicals and its attacks on organics, their fragmentation, finally mineralization. AOPs include some kinds of processes such as UV-related oxidation (UV/H_2O_2, UV/chlorination), photocatalysis (UV/TiO_2), and single process that generates hydroxyl radicals (Ozonation, H_2O_2, UV photolysis) (Melin & Hogan, 2000).

AOPs has several advantages. Hydroxyl radical, their reaction species, reacts almost every pollutants because of its strong and nonselective reactivity (Andreozzi, Caprio, Insola, & Marotta, 1999). And AOPs can transform the organics into intermediates, CO_2 and H_2O, and finally mineralize them (Munter, 2001).

Among the various AOP treatments, UV/H_2O_2 is the common treatment in water treatment plant. However, alkalinity and dissolved organic matter in water can scavenge the hydroxyl radical which is main factor in UV/H_2O_2 (Wols, Hofman-Caris, Harmsen, & Beerendonk, 2013). UV/Chlorination is one of the alternatives to UV/H_2O_2, has been reported to be effective for eliminating some Pharmaceuticals and personal care products (PPCPs) (Nam, Yoon, Choi, & Zoh, 2015; Yang et al., 2016).

1.5. Preliminary studies on 1H-benztriazole degradation by AOPs

Degradation characteristics of BTA during AOPs have been studied. There are some studies on degradation of BTA by UV-C/H_2O_2, UV-C/Chlorination, ozonation, and chlorination. Recently, removal and photochemical fate of BTA during sunlight photolysis were studied (Table 3).

By UV-C photolysis, BTA was removed and followed pseudo-first-order kinetics. By adding H_2O_2 solution, generated OH radicals can react with BTA and it follows second order kinetics (8.3×10^9 M^{-1} s^{-1}). And the reaction was pH-dependent, more photo-reactive in the pH condition below pKa, with the deprotonated form (Bahnmueller, Loi,

Linge, Von Gunten, & Canonica, 2015). Among the some UV AOP processes, UV-C/HOCl was the most efficient followed by UV-C/H_2O_2, and UV-C/ClO_2, and the applicability to WWTP and the energy reduction effect of the UV/chlorination process compared to UV/H_2O_2 have also been confirmed (Sichel, Garcia, & Andre, 2011).

There were some studies including about reaction byproducts, or transformation products during the process. Nika et al. studied the degradation of BTA during chlorination, they had examined the removal characteristics of BTA by the molar ratio of free chlorine and BTA, reaction time, solution pH, and with/without TSS co-existence in the solution. And then, they identified reaction intermediates using LC-qTOF-MS and it was confirmed that BTA is produced by chlorination of 1OH-benzotriazole (Nika et al., 2017). Weidauer et al. examine the removal of BTA by simulated sunlight photolysis, identified the transformation products of BTA, and proposed transformation pathways of BTA included aniline and etc. It is confirmed that the transformation products identified in this study were reactive and non-persistent (Weidauer, Davis, Raeke, Seiwert, & Reemtsma, 2016).

1.6. Objectives

Through the previous studies, it is confirmed BTA is not eliminated well by conventional wastewater treatment process, but by AOPs using UV is efficient to BTA removal. Most studies in Table 3 focused on removal kinetics of BTA, some of which included byproducts after the process, but the toxicity of the process had been rarely discussed. However, not only the removal efficiency of process, but the toxic profiles during the process must be considered because some compounds could be changed into more toxic form during the treatments.

Depending on the type of UV source, the profiles of toxicity and byproducts during the treatment can be different. A study on UV photolysis of diclofenac showed that UV-A took more time to completely remove the target compound, but it produced less byproducts and decreased more toxicity than UV-C (Kovacic et al., 2016).

Therefore, the objectives of this study are

1) To determine the removal kinetics of BTA during UV-A/chlorination,

2) To screen the byproducts of BTA and to examine the toxicity change of the samples before and after treatment,

3) To propose the byproducts pathway for BTA during UV-A/chlorination process.

Table 3. Preliminary studies on removal of 1H-benzotriazole during various treatment.

Process	Removal kinetics	Byproducts identification	Toxicity change	Reference
UV/Chlorination	o	x	x	Sichel et al., 2011
Ozonation	o	o	x	Müller et al., 2012
UV photolysis	o	o	o	Benitez, Acero, Real, Roldan, & Rodriguez, 2013
UV photolysis and UV/H_2O_2	o	x	x	Bahnmueller et al., 2015
Membrane filtration and chemical oxidation	o	x	x	Acero, Benitez, Real, & Rodriguez, 2015
UV photocatalysis - UV/TiO_2/Persulfate	o	x	x	Ahmadi, Ghanbari, & Moradi, 2015
UV and ultrasound	o	x	x	Wu, Xu, Bian, Chen, & He, 2016
UV photolysis and UV/H_2O_2	o	o	o	Borowska, Felis, & Kalka, 2016
Wetland + artificial sunlight	o	o	x	Felis, Sochacki, & Magiera, 2016
Biochar	o	x	x	Kim et al., 2016
Sunlight photolysis	o	o	x	Weidauer et al., 2016
Chlorination	o	o	x	Nika et al., 2017

II. Materials and Methods

2.1. Chemicals

Analytical standard of 1H-benzotriazole ($C_6H_5N_3$) was purchased from Sigma-Aldrich (St. Louis, MO, USA). 1H-benzotriazole was dissolved in Deionized water from Milli-Q Water Purification System (Millipore, Burlington, MA, USA) at the concentration of 1000 mg/L. This stock solution was stored in initial condition before the experiments. sodium hypochlorite (NaOCl), formic acid (CH_2O_2), sodium thiosulfate ($Na_2S_2O_3$), potassium hydrogen phthalate ($C_8H_5KO_4$), sodium carbonate (Na_2CO_3), sodium bicarbonate ($NaHCO_3$), acetic acid ($C_2H_4O_2$) and ammonium acetate ($C_2H_7NO_2$) was purchased from Sigma-Aldrich (St. Louis, MO, USA).

Table 4. Physico-chemical properties of 1H-benzotriazole.

Properties		**Structure**
Chemical formula	$C_6H_5N_3$	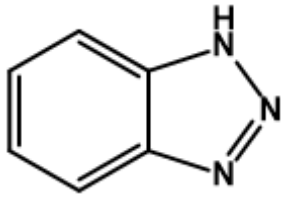
Molecular weight	119.05	
pKa	8.2	
Solubility in water	20 g/L	

2.2. Experimental procedures

2.2.1. Oxidation of benzotriazole

UV photolysis, UV/chlorination, and chlorination experiments were performed using a batch type photoreactor equipped with a mercury lamp (6W, San-Kyo Electrics, Japan) (Figure 1). The emission spectra of mercury lamps were 254 nm (UV-C), 315 nm (UV-B), and 365 nm (UV-A) respectively. The UV intensity of a single lamp was 3.3-4.3 mW/cm^2, which was measured using a radiometer (VLX-3W Radiometer 9811-50, Cole-Parmer, USA). The each UV lamps were stabilized for 30 minutes before starting the experiments.

For UV/chlorination experiments, the BTA standard stock solution was diluted in D.I water at initial concentration. Magnetically stirred, the UV lamp was set into the reactor, right after adding the sodium hypochlorite solution to the reaction solution. For UV photolysis or chlorination experiments, the procedure was same with that of UV/chlorination except for adding sodium chlorite or setting the UV lamp.

The initial concentration of benzotriazole was 1 μM (119 μg/L) for removal kinetics, 100 μM (11.9 mg/L) for by-product identification and ecotoxicity test. The concentration of benzotriazole and free chlorine for byproducts identification and ecotoxicity was set 100 times higher than that for kinetics. It was because high concentration could get stable result with some instrument or test methods. The initial concentration of free chlorine was 25, 50, 75, 100 μM (1.8, 3.6, 5.3, 7.1 mg/L) for kinetics, 5 mM (355 mg/L) for byproducts identification and ecotoxicity test.

All experiments were performed at room temperature (24±1℃). Samples were taken at every specific time. Residual free chlorine was measured by Pocket colorimenter™ II (HACH, Loveland, CO, USA) at some sampling time. pH buffer solution was not used for excepting the reaction between reactants and various ions in buffer solution. The initial pH was adjusted at 6.7, with 1M sulfuric acid and 1M sodium hydroxide, and pH was measured at some sampling time by NeoMet pH/ORP meter pH-220L (iSTEK, Korea).

2.2.2. Ecotoxicity test

Ecotoxicity of untreated and treated samples were tested by Microtox Model 500 Toxicity Analyzer. Using the bioluminescent bacterium *Vibrio Fischeri*, the bioluminescence inhibition of the samples was measured. The tests were performed following the protocol - 81.9% basic test. Samples taken for toxicity test were dechlorinated with sodium thiosulfate and the pH was adjusted to 6-8 with HCl and NaOH to provide a stable condition for the bacteria.

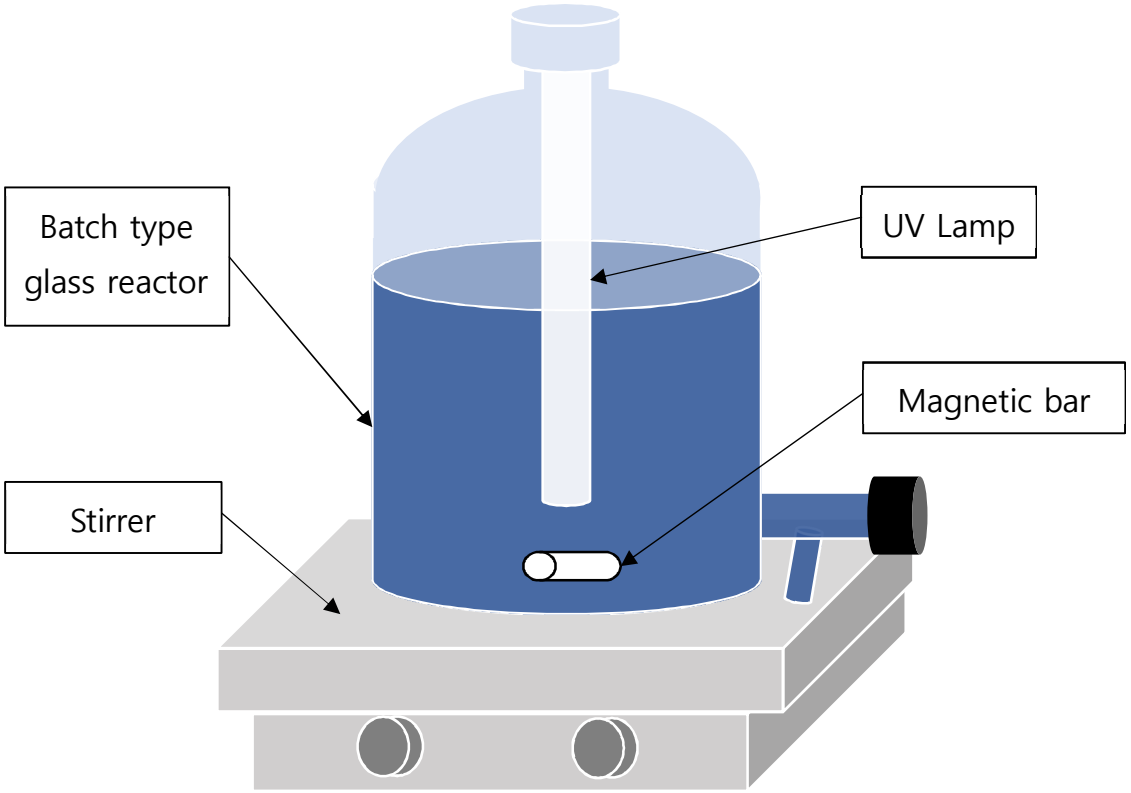

Figure 1. The schematic of the photolysis reactor batch system.

2.3. Analytical methods

2.3.1. UHPLC-MS/MS

To examine BTA removal during the oxidation processes, UHPLC (Nexera, Shimadzu, Kyoto, Japan) equipped with tandom mass spectrometer (API 4000, AB Sciex, USA) was used.

BTA was analyzed with Luna® Phenyl-Hexyl column, 3 μm particle size, 150 x 4.6 mm (Phenomenex, Torrance, CA, USA). The analysis was performed in isocratic mode with 0.1% formic acid in water as mobile phase A and methanol as mobile phase B, at a flow rate of 0.3 mL/min and column temperature of 30℃.

Electrospray ionization (ESI) was used in positive mode, and MRM (Multi Reaction Monitoring) mode was used to detect BTA. The MRM method of BTA is described in Table 5.

Table 5. The MRM method of 1H-benzotriazole for LC-MS/MS.

Precursor ion (m/z) (Da)	Product ion (m/z) (Da)	Declustering potential (volts)	Collision energy (volts)	Collision cell exit potential (volts)
120	65	36	31	6
120	92	36	23	8

2.3.2. UPLC-qTOF-MS

UPLC-qTOF-MS was used for screening and identifying the reaction byproducts of benzotriazole during UV/chlorination process. A Waters ACQUITY UPLC system connected to Synapt G2-S equipped with an electrospray ionization source (Waters corporation, Milford, MA, USA). The methods and MS parameters were referred and modified from Weidauer et al., 2016. Analytes were separated on a Kinetex C18 column (100 mm x 2.1 mm, 1.7 μm) at a flow rate of 0.45 mL/min and a column temperature of 60℃. The injection volume was 10 μL. Two different LC method were applied (Table 6).

Table 6. LC conditions for by-products analysis.

	Method 1		Method 2	
Mobile phase A	Water with 0.1% formic acid		1 mM ammonium acetate with 0.05% acetic acid, pH 5	
Mobile phase B	MeOH with 0.1% formic acid		1 mM ammonium acetate in MeOH with 0.05% acetic acid, pH 5	
Gradient mode	Time (min)	B (%)	Time (min)	B (%)
	0.0	1.0	0.00	2.0
	12.25	99.0	12.25	98.0
	13.00	99.0	13.00	98.0
	13.01	1.0	13.01	2.0
	15.00	1.0	15.00	2.0

Samples were analyzed in positive and negative ion mode, with MSe method (continuum for screening with UNIFI; centroid for identification with Masslynx). The parameters of HRMS were as follows.

- Capillary voltage 0.7 kV, sampling cone voltage 35 kV, source offset 50 V.
- Source temperature 140℃, desolvation temperature 550℃.
- Desolvation gas flow 950 L/h.

To adjust the value of mass spectra during analysis, leucine enkephalin was used as lock spray and MS calibration using sodium formate was applied in the range of m/z 50 - 750.

Data processing was performed by Masslynx and UNIFI (Waters corporation, Milford, MA, USA). With UNIFI, comparing ion chromatogram of treated samples to that of control sample, some unknown unique ion chromatograms were classified with a mass tolerance of 5 ppm. And manual identification was conducted by using Masslynx and ChemDraw 16 (CambridgeSoft, Waltham, MA, USA).

2.3.3. Ion Chromatography

The concentration of formate, chlorite, chlorate, and nitrate ions were measured by ion chromatography (ICS-1100, Dionex, Sunnyvale, CA, USA). For separation of the four anions, an IonPac AG14 guard column (50 × 4 mm) and IonPac AS14 column (250 × 4 mm) were used. To measure nitrate ion, an eluent containing a mixture of 3.5 mM Na2CO3 and 1.0 mM NaHCO3 was used. For the other three anions, a mixture of 2.7 mM Na2CO3 and 1.0 mM NaHCO3 was used as eluent at the flow rate of 1.2 mL/min.

2.3.4. TOC (Total Organic Carbon) analyzer

To confirm the mineralization of the process, untreated and treated samples were analyzed by TOC analyzer (TOC 5000, Shimadzu, Kyoto, Japan).

2.3.5. UV spectrophotometer

Infinite M200 (TECAN, Männedorf, Swiss) was used to scan the absorbance of BTA in the range of UV wavelength. 1, 5, and 10 mg/L of BTA in water was transferred into the cuvette and measured the absorbance for calculating the molar absorption coefficient of BTA.

2.3.6. Hach colorimeter

To measure residual free chlorine, portable colorimeter II was used. It can measure a concentration of until 8 mg/L as Cl_2, the samples expected over 8 mg/L were diluted with

D.I. water.

III. Results and discussion

3.1. Removal efficiencies of 1H-benzotriazole by different UV wavelength

Removal efficiencies of BTA during UV photolysis by different UV wavelength were examined at UV-A (365 nm), B (315 nm), and C (254 nm) range. BTA was removed well during UV-C photolysis, partly removed during UV-B photolysis, and not removed well during UV-A photolysis in 180 min. During UV-C photolysis, about 99.9% of BTA was removed within 90min, however, with UV-B and UV-A, about 48.7% and 4.1% of BTA was removed within 180 min (Figure 2).

Removal efficiency during UV photolysis depends on the molar absorption coefficient of the compounds in irradiated wavelength. Figure 3 shows the molar absorption coefficient of BTA in the UV wavelength of 230-400 nm. Its molar absorption coefficient has a trend rapidly increasing at from 230 nm to 260 nm and decreasing until 300 nm, and keeps decreasing, with almost 0 m^2/mol, to 400 nm. Higher molar absorption coefficient means that BTA absorb more UV light at that wavelength, can react more actively, and can be resulted faster reaction rate. The result about removal efficiency can be explained with the result about molar absorption coefficient.

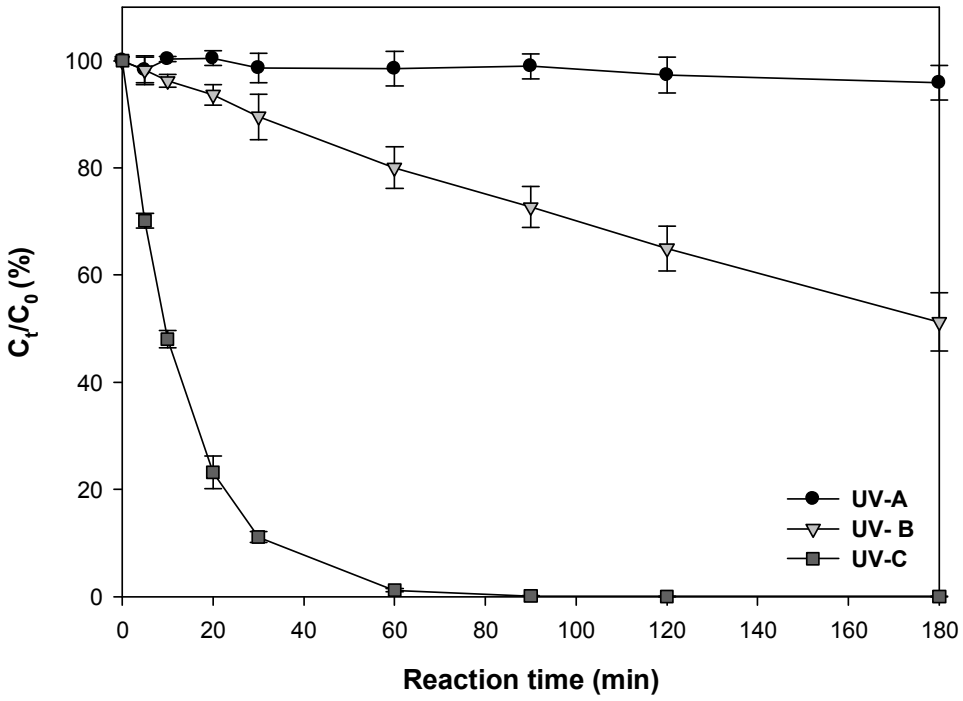

Figure 2. BTA removal during UV photolysis.

($[BTA]_0$ = 1 μM, UV-A = 365 nm, UV-B = 312 nm, UV-C = 254 nm)

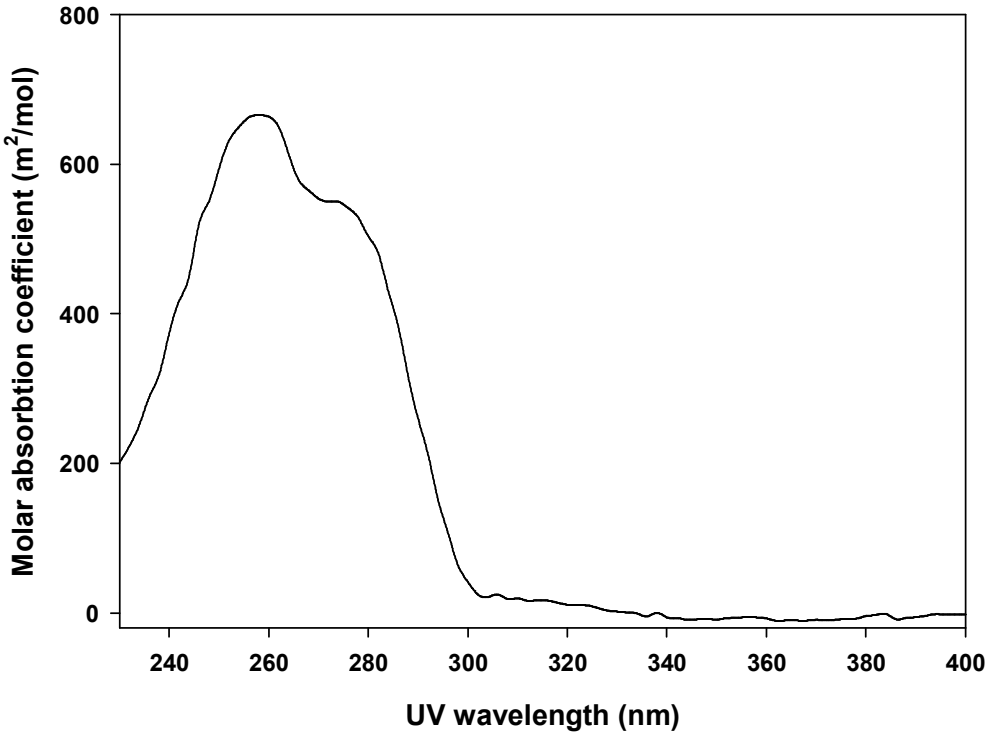

Figure 3. Molar absorption coefficient of 1H-benzotriazole based on the UV wavelength (230 nm-400 nm).

3.2. Degradation kinetics of 1H-benzotriazole during UV-photolysis, chlorination, and UV/chlorination process

Removal efficiencies of BTA during UV-A photolysis, chlorination, and the combination process were investigated (Figure 4). In each of single process, BTA was hardly removed, however, in the combination process of them, BTA was effectively eliminated within 180 min.

Free chlorine, injected in the form of NaOCl, is presented in water in the forms of HOCl or OCl^- depending on the pH. Both of them can generate OH radical, when they were irradiated by UV, which is highly reactive.

The mechanisms of OH radical generation is as follows (Fang, Fu, & Shang, 2014).

$HOCl \rightleftarrows OCl^- + H^+$ (pKa 7.6) (Eq 1.)

$HOCl + UV\ photon \longrightarrow \bullet OH + \bullet Cl$ (pH < 7.6 at 25℃) (Eq 2.)

$OCl^- + UV\ photon \longrightarrow \bullet O^- + \bullet Cl$ (Eq 3.)

$\bullet O^- + H_2O \longrightarrow \bullet OH + OH^-$ (pH > 7.6 at 25℃) (Eq 4.)

It could be seen that direct photolysis by UV-A was insufficient for BTA degradation, indirect photolysis by OH radical, generated by reaction between $HOCl/OCl^-$ and UV photon, was effective for BTA removal.

The expected mechanisms of BTA degradation is as follows.

BTA + UV photon → products (Eq 5.)

BTA + • OH → products, $k = 2.0 \times 10^9 M^{-1}s^{-1},\ 8.3 \times 10^9\ M^{-1}s^{-1}$

(Bahnmueller et al., 2015; Borowska et al., 2016) (Eq 6.)

BTA + • Cl → products (Eq 7.)

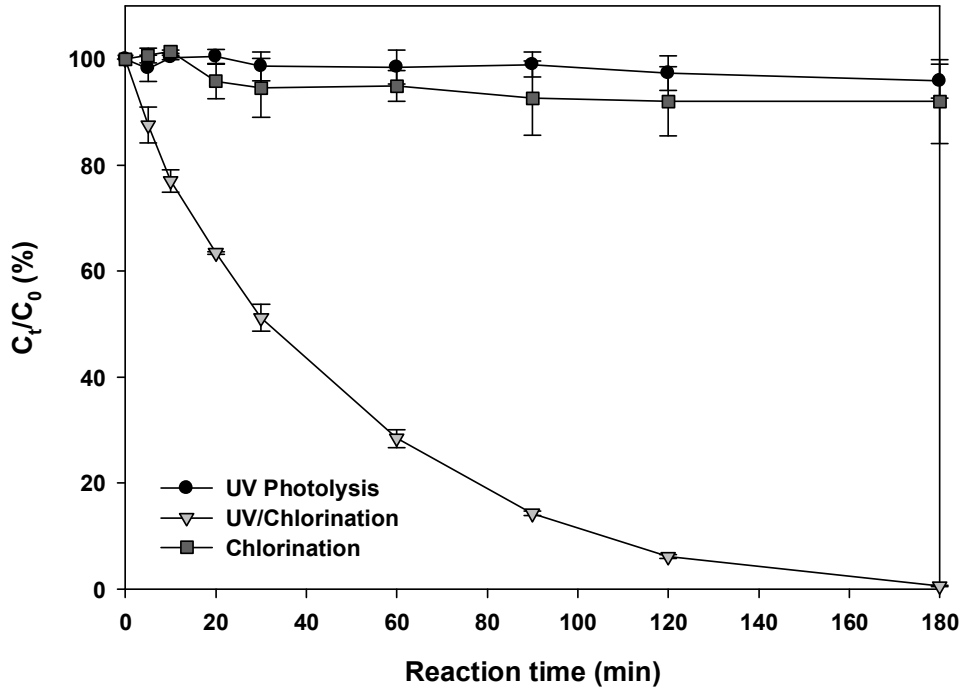

Figure 4. BTA removal during UV photolysis, chlorination, and UV/chlorination. ($[BTA]_0$= 1 μM, $[Cl_2]_0$ = 25 μM (1.8 mg/L), UV wavelength = 365 nm, n=3)

3.3 Degradation kinetics of 1H-benzotriazole during UV-A/chlorination depends on chlorine dosage and pH

It was observed that there was synergy effect between UV-A and free chlorine for BTA degradation in 3.2. After then, all subsequent experiments were performed at 365 nm of UV wavelength.

Firstly, degradation kinetics depending on chlorine dosage was examined. The experiments were conducted at initial BTA concentration of 1 μM (119 μg/L), and the initial free chlorine concentrations of 25, 50, 75, 100 μM (1.8, 3.6, 5.3, 7.1 mg/L as Cl_2). The reaction follows pseudo-first order kinetics and chlorine dosage affected to degrade BTA during UV-A/chlorination (Figure 5, Table 7). The radicals generated by irradiation of free chlorine was estimated as the main factor for BTA degradation during UV/chlorination, and the more chlorine dosage can generate more radicals. Therefore, the chlorine dosage affected positively to BTA degradation during UV/chlorination.

Secondly, effect of pH during UV/chlorination was investigated. The experiments were performed at various pH conditions of pH 3, 5, 7, 9 with not buffered solution, but pH adjusted with H_2SO_4 or NaOH. The higher reaction rates were calculated at the condition in the orders of pH 9, 5, 3, and 7.

According to Eq 1, free chlorine was presented in solution in the forms of HOCl or OCl^-. As the form of chlorine, radical species generated and their amount, and UV wavelength that they mainly absorb were different. HOCl, the main form in acidic solution below pH 7.6, is rapidly react with UV and generate OH radical(hydroxyl radical), and OCl^- is the main form in basic solution over pH 7.6, generate hydroxyl radical but also scavenge the hydroxyl radical. However, in the range of UV-A wavelength, OCl^- absorbs much more light than HOCl (Remucal & Manley, 2016).

UV/chlorination produces primary radicals described in eqs 1-4, in 3.2, and also secondary radicals such as ClO•. The related equations are as follows (Fang et al., 2014; Guo et al., 2017; Sun, Lee, Zhang, & Huang, 2016; Z. Wu et al., 2016).

• $Cl + Cl^- \underset{\leftarrow (k_2)}{\overset{\rightarrow (k_1)}{}} Cl_2^{\bullet-}$, $k_1 = 6.5 \times 10^9\ M^{-1}s^{-1}$, $k_2 = 1.1 \times 10^5\ s^{-1}$ (Eq 8.)

• $OH + HOCl \rightarrow ClO\bullet + H_2O$, $k = 2.0 \times 10^9\ M^{-1}s^{-1}$ (Eq 9.)

• $OH + OCl^- \rightarrow ClO\bullet + OH^-$, $k = 8.8 \times 10^9\ M^{-1}s^{-1}$ (Eq 10.)

• $Cl + HOCl \rightarrow ClO\bullet + H^+ + Cl^-$, $k = 3.0 \times 10^9\ M^{-1}s^{-1}$ (Eq 11.)

• $Cl + OCl^- \rightarrow ClO\bullet + H^+ + Cl^-$, $k = 8.2 \times 10^9\ M^{-1}s^{-1}$ (Eq 12.)

The affecting radicals were significantly different according to the structure of target compounds. The compounds containing benzene ring attached with electron-rich functional groups were affected more by the reactive chlorine species (RCS), such as ClO•, and $Cl_2^{\bullet-}$, than • OH. By these equations above, the concentration of • OH, • Cl, and $Cl_2^{\bullet-}$ are decreased and that of ClO• kept constant with increasing pH. Additionally, the concentration of ClO• is about 10^4 times higher than those of the others (Chuang, Chen, Chinn, & Mitch, 2017; Guo et al., 2017).

Therefore, in acidic pH, hydroxyl radical was mainly produced from HOCl and would react with BTA, in neutral pH, similar to acidic condition, however the scavenging effect of OCl^- was added resulting lower reaction rate than that in acidic condition. In basic pH, chlorine was mainly presented in the form of OCl^-, rapidly convert to ClO•, ultimately the RCS reacted with BTA.

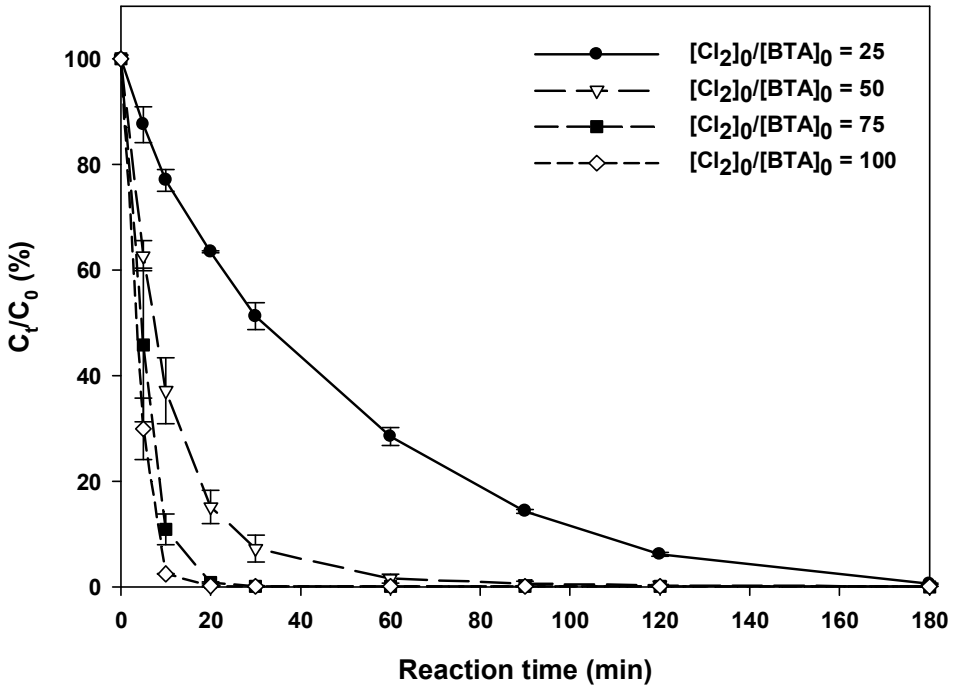

Figure 5. Removal of 1H-benzotriazole during UV/chlorination process with the different chlorine dosages. ($[BTA]_0$ = 1 μM (119 ug/L); $[Cl_2]_0$ = 25, 50, 75, 100 μM (1.8, 3.6, 5.3, 7.1 mg/L as Cl_2); UV wavelength = 365 nm, n=2)

Table 7. The pseudo-first order rate constants and coefficient of determination by various chlorine dosage.

$[Cl_2]_0/[BTA]_0$	25	50	75	100
k (min^{-1})	0.0225	0.0882	0.234	0.3405
R^2	0.9963	0.9963	0.9956	0.9869

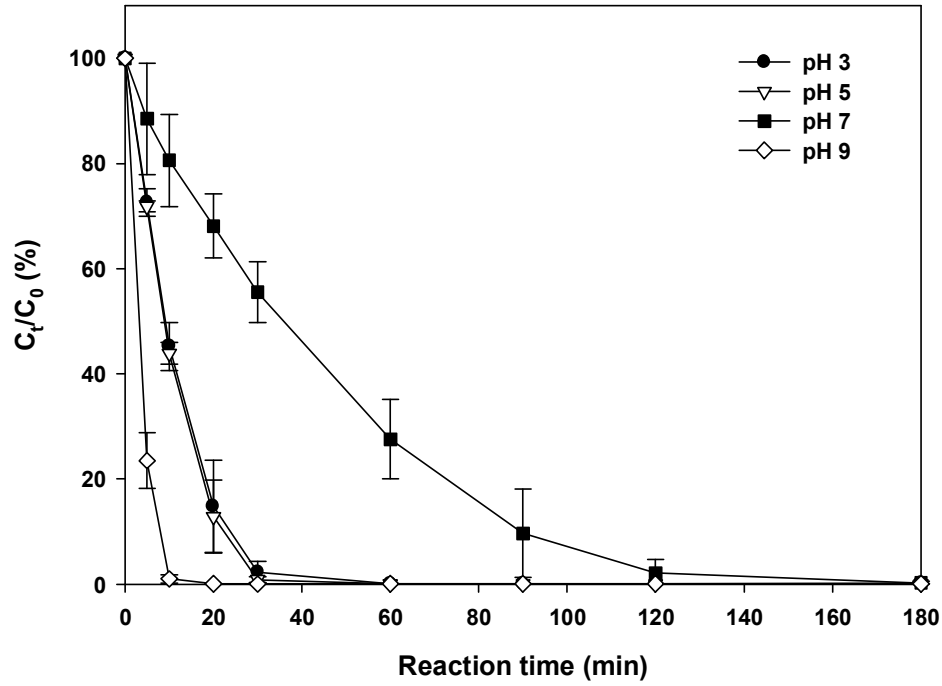

Figure 6. Removal of 1H-benzotriazole during UV/chlorination process with the different pH. ($[BTA]_0$ = 1 μM (119 ug/L); $[Cl_2]_0$ = 50 μM (3.6 mg/L); UV wavelength = 365 nm; pH was adjusted with H_2SO_4 and NaOH solution, n=2)

Table 8. The pseudo-first order rate constants and coefficient of determination by various pH condition.

pH	**3.0**	**5.0**	**7.0**	**9.0**
k (min^{-1})	0.1213	0.1388	0.0212	0.4103
R^2	0.9912	0.9743	0.9964	0.9722

3.4 Mineralization and identification of byproducts of 1H-benzotriazole during UV/chlorination

Mineralization of BTA during UV/chlorination was confirmed by TOC analyzer and IC. Considering the quantitation range of these instruments, experiments for mineralization were performed with 100 times higher concentration of BTA and free chlorine, than those for kinetics.

As BTA was eliminated during the reaction, TOC was decreased with similar pattern. For 12 hours reaction, almost 50% of BTA was mineralization during UV/chlorination. It means that about 50% of degraded BTA was mineralized, and the other 50% was transformed and remained other forms of organic compounds. And two related ion byproducts were detected, formate ion and nitrate ion. As the 50% of carbon in BTA was mineralized, about 5 % of carbon was converted into formate ion (Figure 7). Formate ion can be further mineralized to carbon dioxide by the reaction with hydroxyl radical (Eq 13, 14) (Lee, Lee, & Yoon, 2004).

$$HCOO^- + \bullet OH \rightarrow \bullet CO_2^- + H_2O \quad \text{(Eq 13.)}$$

$$\bullet CO_2^- + O_2 + H^+ \rightarrow CO_2 + HO_2\bullet \quad \text{(Eq 14.)}$$

Also 9% of nitrogen in BTA was mineralized and detected in the form of nitrate ion. It was reported that nitrate ion can be produced in advanced oxidation process of nitrogen containing compounds like chlorophenols (Trapido, Veressinina, & Kallas, 2001).

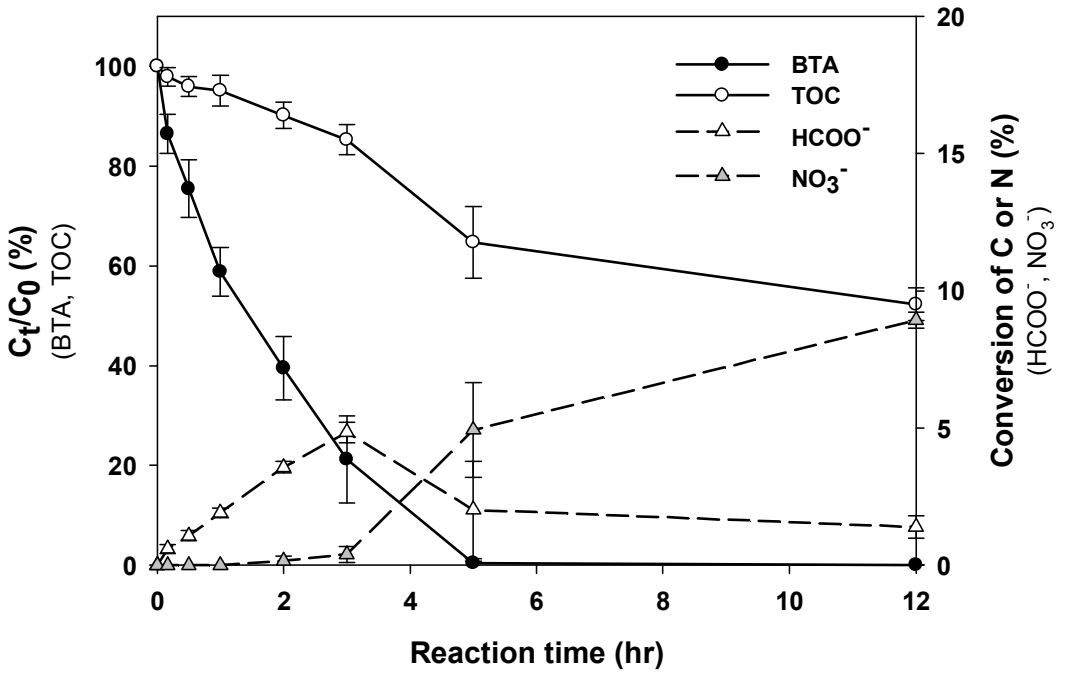

Figure 7. Time profiles of the 1H-benzotriazole, TOC (Total Organic Carbon), formate and nitrate ions during UV/chlorination.

($[BTA]_0$ = 100 μM (11.9 mg/L); $[Cl_2]_0$ = 5 mM (355 mg/L); UV wavelength = 365 nm)

In UV/chlorination process, chlorinated disinfection byproducts can be formed and two chlorinated ions were detected. Figure 8 shows the formation of chlorite and chlorate ion during UV/chlorination. During the process, as the free chlorine react with UV and BTA, chlorite ion was initially produced and then eliminated all after 5 hr. In the case of chlorate, it was gradually increased until the chlorite reacted and removed all. Finally about 23% of injected chlorine were converted to chlorate ion.

The final products of OCl^- during UV-A photolysis are O_2, Cl^-, ClO_2^- and ClO_3^-. And the related equation as follows (Eq 15-19). Among them chlorite and chlorate need to be considered, because of their adverse health effect (Buxton & Subhani, 1972; Wang, 2015).

$OCl^- + hv \rightarrow Cl^- + O(^3P)$ $(\lambda > 320\ nm)$ (Eq 15.)

$O(^3P) + OCl^- \rightarrow ClO_2^-$ (Eq 16.)

$O(^3P) + OCl^- \rightarrow Cl^- + O_2$ (Eq 17.)

$O(^3P) + ClO_2^- \rightarrow ClO_3^-$ (Eq 18.)

$O(^3P) + ClO_2^- \rightarrow Cl^- + O_2 + O(^3P)$ (Eq 19.)

The concentration of chlorite and chlorate in drinking water was regulated by WHO, at the concentration of 0.7 mg/L.

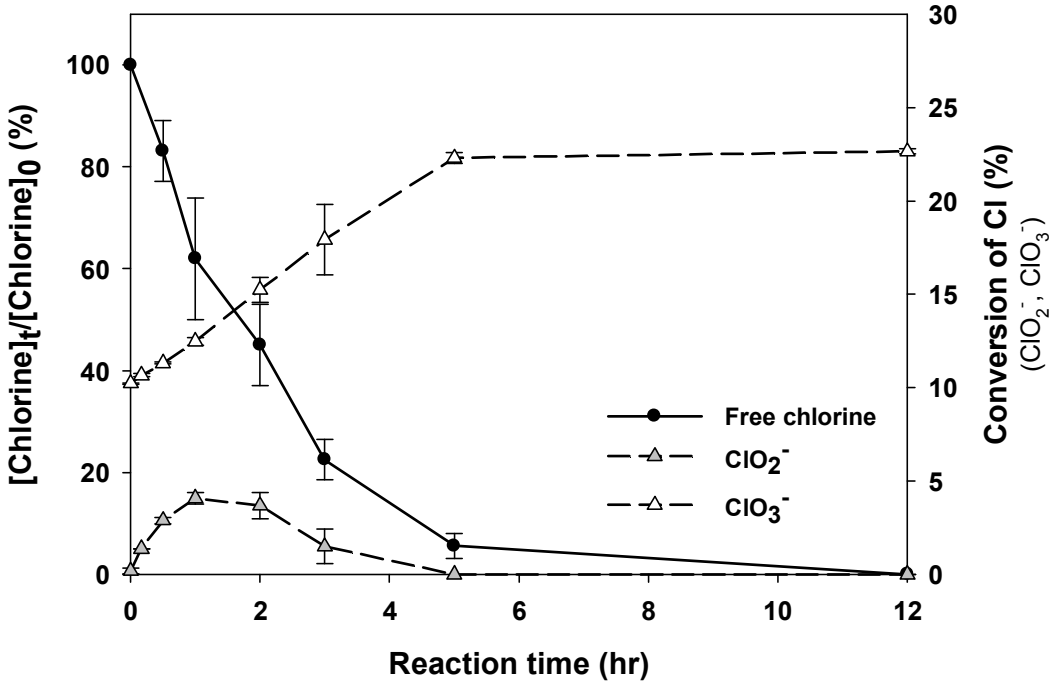

Figure 8. Formation of chlorite and chlorate ion during UV/chlorination of BTA. ($[BTA]_0$ = 100 μM (11.9 mg/L); $[Cl_2]_0$ = 5 mM (355 mg/L); UV wavelength = 365 nm)

Five organic byproducts (m/z 150.0307, 166.0252, 124.0147, 140.0071, 154.0245) of BTA during UV/chlorination were identified using UPLC-qTOF-MS (Table 9). Byproduct1, Byproduct2, and Byproduct3 were detected in negative mode, and Byproduct4 and Byproduct5 were detected in positive mode.

Figure 9 shows the profiles of byproducts during UV/chlorination, the peak area of Byproduct3 was the highest, following by Byproduct4. Among them, Byproduct1, Byproduct2, and Byproduct3 had a trend that increasing until specific points and then decreasing. However, Byproduct4 and Byproduct5 continued to increase until BTA was removed about 100%.

Using identified byproducts and their profile, The degradation pathway of BTA during UV/chlorination was proposed in Figure 9. The basic mechanism was referred from "The UV/oxidation hand book (SES, 1994)". The main mechanisms of BTA degradation during UV/chlorination, were hydroxylation, ring opening, and electron transfer by reaction with OH radical.

For Byproduct1 with an accurate mass of 150.0307 m/z $[M-H]^-$, a structure with open benzene ring with addition of two atoms of oxygen was suggested. Byproduct2, which differs from Byproduct1 by one atom of oxygen, could be explained the structure of it with addition of one more atom of oxygen to Byproduct1. Also, Byproduct2 was already proposed from previous research on BTA during UV/H_2O_2 process as one of transformation products of BTA (Borowska et al., 2016). In the case of Byproduct3, with

an accurate mass of 124.0147 m/z $[M-H]^-$, suggested the chemical formula of $C_4H_3N_3O_2$ by 'Elemental composition', an aliphatic structure that is opened benzene and triazole ring with bond scission and is added two atom of oxygen was proposed.

Similarly, for Byproduct4 and Byproduct5, structures that was opened all of rings, was cut one or two of bonds, and was added three atoms of oxygen were suggested.

Table 9. Result of mass fragment analysis about five identified by-products.

Name	RT (min)	m/z (mass accuracy)	adduct	Predicted formula	Fragments m/z (mass error)	Major fragments	Predicted structure
Byproduct 1	0.81	150.0307 (-2.0 ppm)	-H	$C_6H_5N_3O_2$	122.0339 (-1.5 mDa)	$[M-H-CO]^-$	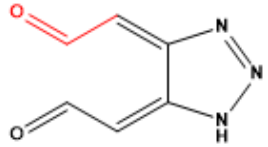
Byproduct 2	1.13	166.0252 (0.6 ppm)	-H	$C_6H_5N_3O_3$	138.0300 (-0.4 mDa) 122.0340 (-1.4 mDa)	$[M-H-CO]^-$ $[M-H-CO_2]^-$	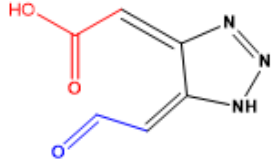
Byproduct 3	1.02	124.0147 (0.0 ppm)	-H	$C_4H_3N_3O_2$	59.0131 (+1.1 mDa) 68.0251 (-1.1 mDa)	$[M-H-C_4HO]^-$ $[M-H-N_3O]^-$	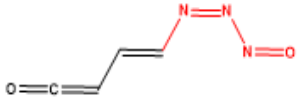
Byproduct 4	0.86	140.0071 (0.7 ppm)	+Na	$C_2H_3N_3O_3$	112.0114 (-0.9 mDa)	$[M+Na-CO]^+$	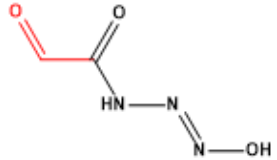
Byproduct 5	0.86	154.0245 (-10.4 ppm)	+Na	$C_3H_5N_3O_3$	96.0165 (-0.9 mDa) 136.0136 (+1.3 mDa)	$[M+Na-C_2H_2O_2]^+$ $[M+Na-H_2O]^+$	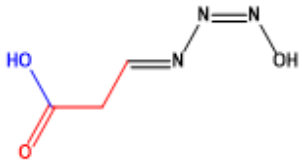

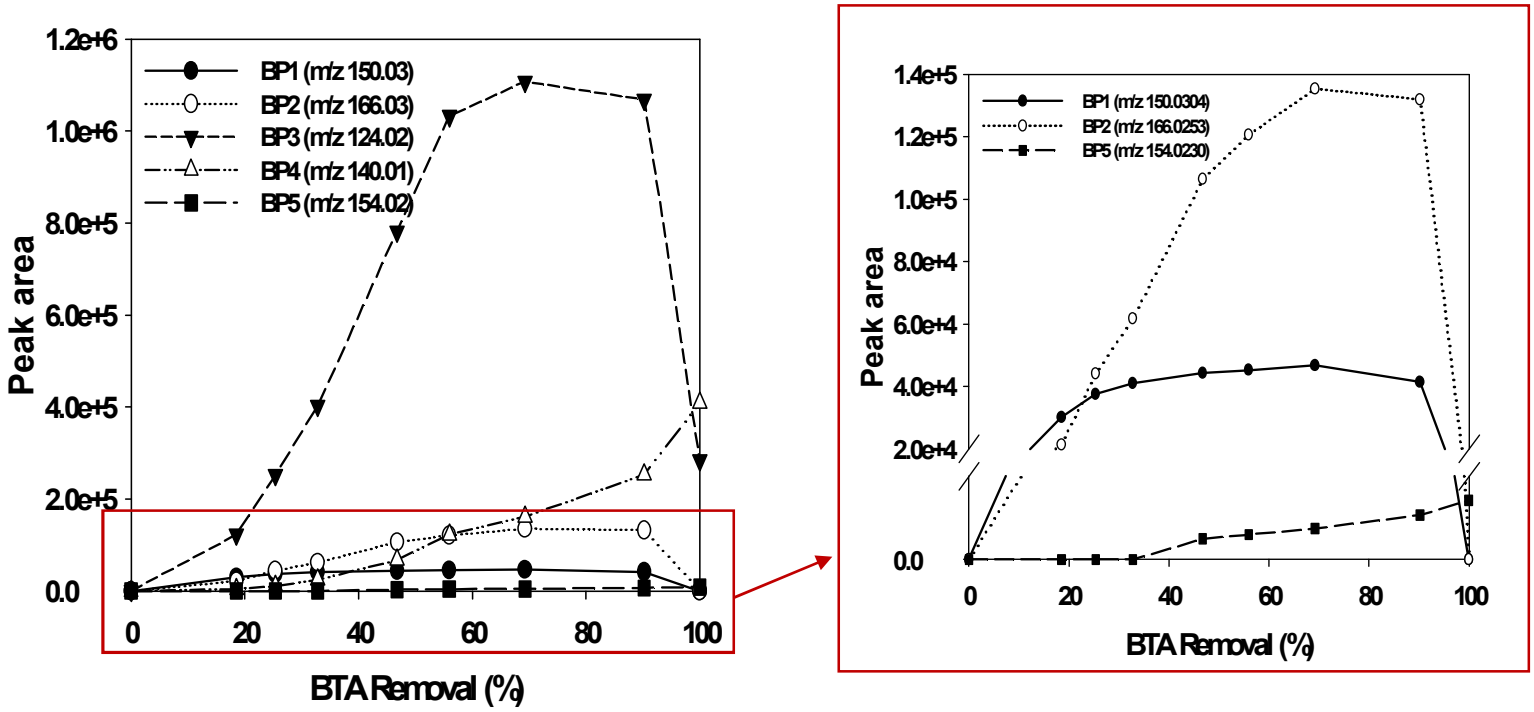

Figure 9. Profiles of byproducts of BTA during UV/chlorination.

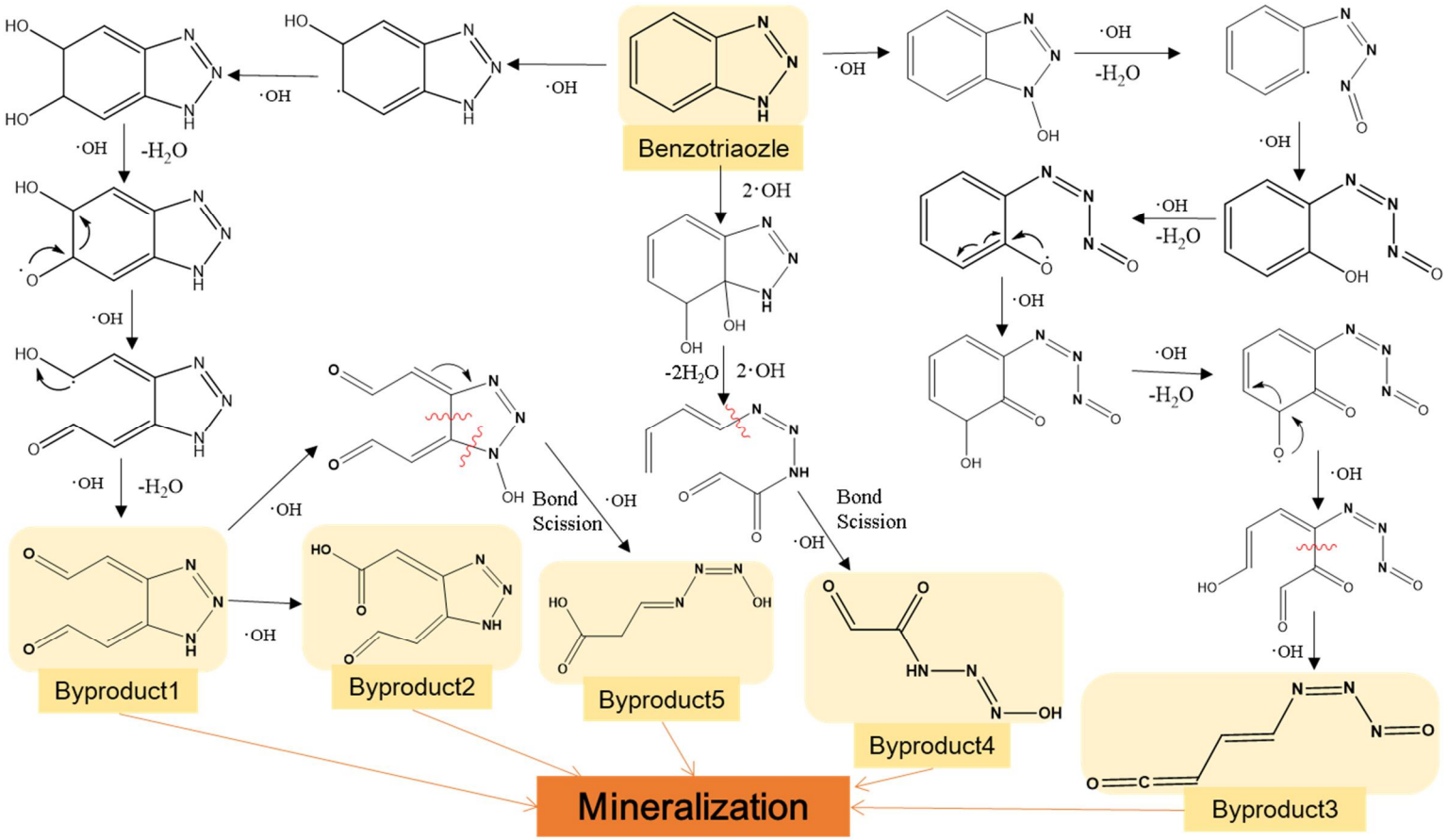

Figure 10. Proposed degradation pathway of BTA during UV-chlorination.

3.5 Toxic profiles during UV/chlorination of 1H-benzotriazole

Toxic profiles during the process were measured by Microtox analyzer. Untreated and treated samples were exposed into activated *Vibrio Fischeri* for 15 min, and the TU (Toxic Unit) of each samples by using measured values of EC50%. If EC50 could not be calculated because the bioluminescence inhibition was less than 10% in the raw water (100%), its TU value was considered as zero (Figure 11).

As the BTA was removed by UV/chlorination, the values of TU of each exposure time were decreased initially until 60 min, increased at 120 min, and decreased again at 300 min. It is estimated that the toxicity increased at 120 minutes when the by-product was most abundant, and then decreased as the byproduct decomposed.

In previous studies, toxic effects of BTA were decreased by 20% during UV photolysis, which resulted in TU decrease from the value of 0.94 to 0.64 before and after the treatment, and during UV/H_2O_2, TU was decreased from 1.07 to 0.28 (Borowska et al., 2016). In another case, the toxic profiles during UV photolysis of BTA had similar trend to this study, with the light inhibition of the bacterium increased at initial period and then decreased after BTA was considerably degraded (Benitez et al., 2013).

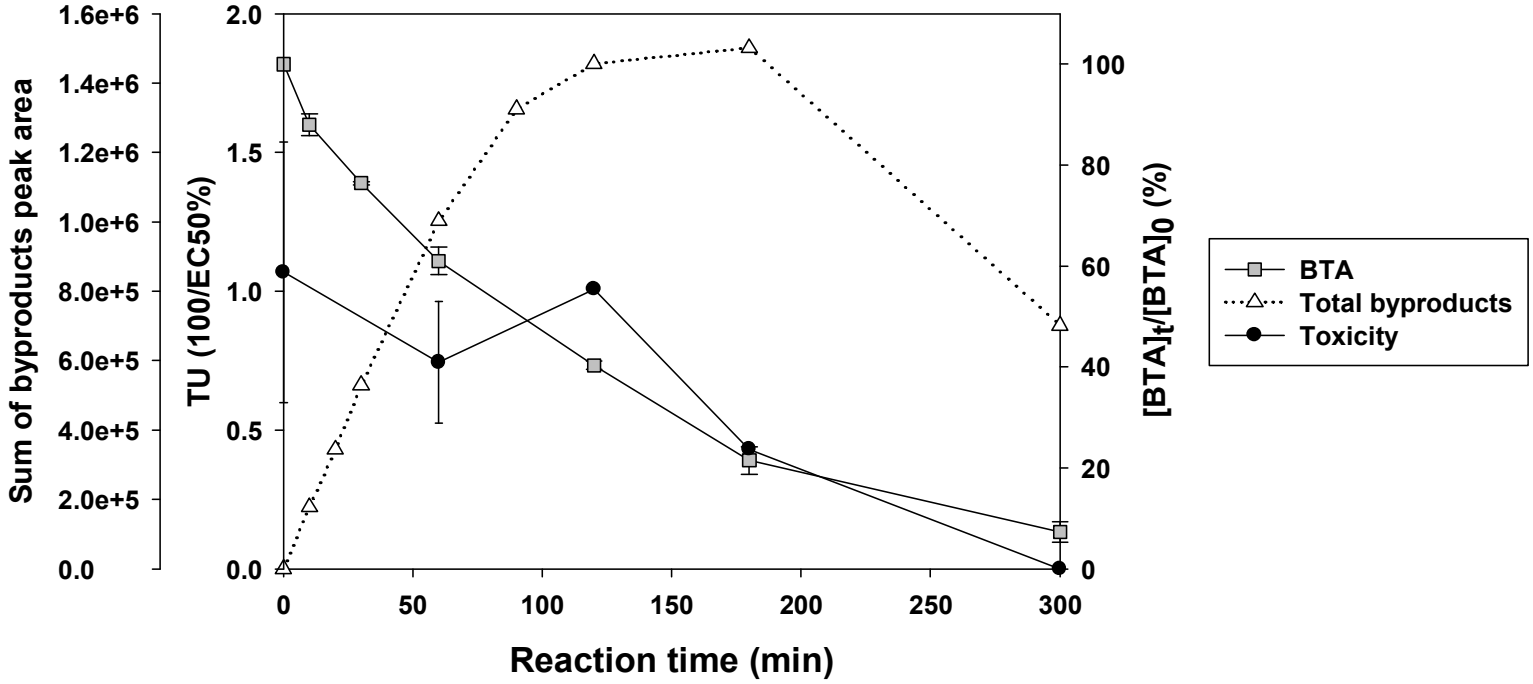

Figure 11. Profiles of BTA, total byproducts, and toxicity during UV/chlorination of BTA.

($[BTA]_0$ = 100 μM (11.9 mg/L); $[Cl_2]_0$ = 5 mM (355 mg/L); UV wavelength = 365 nm)

IV. Conclusion

In this study, degradation efficiencies of benzotriazole during UV photolysis and UV/chlorination were investigated. For UV-A, only photolysis was not effective to remove BTA, however, with chlorine together, which seemed also not effective alone, could remove BTA effectively for 180 min. This synergetic effect is due to the OH radical generated in the UV/chlorination process. For UV-A/chlorination, alkaline pH, where free chlorine is presented in the form of OCl^-, increased the reaction rate of BTA.

During the UV/chlorination process, BTA was mineralized about 50% and it means BTA was transformed in other forms of organic compounds. Therefore, four ion byproducts ($HCOO^-$, NO_3^-, ClO_2^-, ClO_3^-) and five organic byproducts (m/z 150.0307, 166.0252, 124.0147, 140.0071, 154.0245) of BTA during UV/chlorine process were identified. Using the identified byproducts, the degradation pathway of BTA was proposed. Also, Toxicity profiles during UV-A/chlorination of BTA was examined, the toxicity was increased at first, and decreased as the reaction ended.

BTA was effectively removed and partly mineralized during UV-A/chlorination. And its toxic effect to ecosystem was decreased. Therefore, UV-A/chlorination could be an option to improve removal efficiency of water treatment plants, not only eliminating non-biodegradable compounds, but also reducing its toxicity.

References

Acero, J. L., Benitez, F. J., Real, F. J., & Rodriguez, E. (2015). Elimination of selected emerging contaminants by the combination of membrane filtration and chemical oxidation processes. *Water, Air, & Soil Pollution, 226*(5), 139.

Ahmadi, M., Ghanbari, F., & Moradi, M. (2015). Photocatalysis assisted by peroxymonosulfate and persulfate for benzotriazole degradation: effect of pH on sulfate and hydroxyl radicals. *Water Science and Technology, 72*(11), 2095-2102.

Andreozzi, R., Caprio, V., Insola, A., & Marotta, R. (1999). Advanced oxidation processes (AOP) for water purification and recovery. *Catalysis today, 53*(1), 51-59.

Bahnmueller, S., Loi, C. H., Linge, K. L., Von Gunten, U., & Canonica, S. (2015). Degradation rates of benzotriazoles and benzothiazoles under UV-C irradiation and the advanced oxidation process UV/H 2 O 2. *Water research, 74*, 143-154.

Benitez, F. J., Acero, J. L., Real, F. J., Roldan, G., & Rodriguez, E. (2013). Photolysis of model emerging contaminants in ultra-pure water: kinetics, by-products formation and degradation pathways. *Water research, 47*(2), 870-880.

Borowska, E., Felis, E., & Kalka, J. (2016). Oxidation of benzotriazole and benzothiazole in photochemical processes: Kinetics and formation of transformation products. *Chemical Engineering Journal, 304*, 852-863.

Buxton, G., & Subhani, M. (1972). Radiation chemistry and photochemistry of oxychlorine ions. Part 2.—Photodecomposition of aqueous solutions of hypochlorite ions. *Journal of the Chemical Society, Faraday Transactions 1: Physical Chemistry in Condensed Phases, 68*, 958-969.

Chuang, Y.-H., Chen, S., Chinn, C., & Mitch, W. A. (2017). Comparing the UV/monochloramine and UV/free chlorine Advanced Oxidation Processes (AOPs) to the UV/hydrogen peroxide AOP Under Scenarios Relevant to Potable Reuse. *Environmental Science & Technology*.

Duan, Z., Xing, Y., Feng, Z., Zhang, H., Li, C., Gong, Z., . . . Sun, H. (2017). Hepatotoxicity of benzotriazole and its effect on the cadmium induced toxicity in zebrafish

Danio rerio. *Environmental pollution, 224*, 706-713.

Esteban, S., Gorga, M., Petrovic, M., González-Alonso, S., Barceló, D., & Valcárcel, Y. (2014). Analysis and occurrence of endocrine-disrupting compounds and estrogenic activity in the surface waters of Central Spain. *Science of the Total Environment, 466*, 939-951.

Fang, J., Fu, Y., & Shang, C. (2014). The roles of reactive species in micropollutant degradation in the UV/free chlorine system. *Environmental Science & Technology, 48*(3), 1859-1868.

Felis, E., Sochacki, A., & Magiera, S. (2016). Degradation of benzotriazole and benzothiazole in treatment wetlands and by artificial sunlight. *Water research, 104*, 441-448.

Fent, K., Chew, G., Li, J., & Gomez, E. (2014). Benzotriazole UV-stabilizers and benzotriazole: antiandrogenic activity in vitro and activation of aryl hydrocarbon receptor pathway in zebrafish eleuthero-embryos. *Science of the Total Environment, 482*, 125-136.

Giannakis, S., Vives, F. A. G., Grandjean, D., Magnet, A., De Alencastro, L. F., & Pulgarin, C. (2015). Effect of advanced oxidation processes on the micropollutants and the effluent organic matter contained in municipal wastewater previously treated by three different secondary methods. *Water research, 84*, 295-306.

Giger, W., Schaffner, C., & Kohler, H.-P. E. (2006). Benzotriazole and tolyltriazole as aquatic contaminants. 1. Input and occurrence in rivers and lakes. *Environmental Science & Technology, 40*(23), 7186-7192.

Glaze, W. H., Kang, J.-W., & Chapin, D. H. (1987). The chemistry of water treatment processes involving ozone, hydrogen peroxide and ultraviolet radiation.

Guo, K., Wu, Z., Shang, C., Yao, B., Hou, S., Yang, X., . . . Fang, J. (2017). Radical Chemistry and Structural Relationships of PPCP Degradation by UV/Chlorine Treatment in Simulated Drinking Water. *Environmental Science & Technology, 51*(18), 10431-10439.

Hart, D., Davis, L., Erickson, L., & Callender, T. (2004). Sorption and partitioning parameters of benzotriazole compounds. *Microchemical Journal, 77*(1), 9-17.

Heeb, F., Singer, H., Pernet-Coudrier, B., Qi, W., Liu, H., Longrée, P., . . . Berg, M. (2012). Organic micropollutants in rivers downstream of the megacity Beijing: sources and mass fluxes in a large-scale wastewater irrigation system. *Environmental*

Science & Technology, 46(16), 8680-8688.

Kim, E., Jung, C., Han, J., Her, N., Park, C. M., Jang, M., . . . Yoon, Y. (2016). Sorptive removal of selected emerging contaminants using biochar in aqueous solution. *Journal of Industrial and Engineering Chemistry, 36*, 364-371.

Kiss, A., & Fries, E. (2009). Occurrence of benzotriazoles in the rivers Main, Hengstbach, and Hegbach (Germany). *Environmental Science and Pollution Research, 16*(6), 702-710.

Kovacic, M., Perisic, D. J., Biosic, M., Kusic, H., Babic, S., & Bozic, A. L. (2016). UV photolysis of diclofenac in water; kinetics, degradation pathway and environmental aspects. *Environmental Science and Pollution Research, 23*(15), 14908-14917.

Lee, Y., Lee, C., & Yoon, J. (2004). Kinetics and mechanisms of DMSO (dimethylsulfoxide) degradation by UV/H 2 O 2 process. *Water research, 38*(10), 2579-2588.

Leonards, P., & Lamoree, M. Network of reference laboratories and related organisations for monitoring and bio-monitoring of emerging environmental pollutants.

Liang, X., Martyniuk, C. J., Zha, J., & Wang, Z. (2016). Brain quantitative proteomic responses reveal new insight of benzotriazole neurotoxicity in female Chinese rare minnow (Gobiocypris rarus). *Aquatic Toxicology, 181*, 67-75.

Liang, X., Zha, J., Martyniuk, C. J., Wang, Z., & Zhao, J. (2017). Histopathological and proteomic responses in male Chinese rare minnow (Gobiocypris rarus) indicate hepatotoxicity following benzotriazole exposure. *Environmental pollution, 229*, 459-469.

Liu, Y.-S., Ying, G.-G., Shareef, A., & Kookana, R. S. (2011). Simultaneous determination of benzotriazoles and ultraviolet filters in ground water, effluent and biosolid samples using gas chromatography–tandem mass spectrometry. *Journal of Chromatography A, 1218*(31), 5328-5335.

Liu, Y.-S., Ying, G.-G., Shareef, A., & Kookana, R. S. (2012). Occurrence and removal of benzotriazoles and ultraviolet filters in a municipal wastewater treatment plant. *Environmental pollution, 165*, 225-232.

Melin, G., & Hogan, T. (2000). Treatment technologies for removal of methyl tertiary butyl ether (MTBE) from drinking water. *Rep. No. NWRI-99-06, National Water*

Research Institute, Center for Groundwater Restoration and Protection, Burlington, Ontario, Canada.

Müller, A., Weiss, S. C., Beißwenger, J., Leukhardt, H. G., Schulz, W., Seitz, W., . . . Weber, W. H. (2012). Identification of ozonation by-products of 4-and 5-methyl-1H-benzotriazole during the treatment of surface water to drinking water. *Water research, 46*(3), 679-690.

Munter, R. (2001). Advanced oxidation processes–current status and prospects. *Proc. Estonian Acad. Sci. Chem, 50*(2), 59-80.

Nam, S.-W., Yoon, Y., Choi, D.-J., & Zoh, K.-D. (2015). Degradation characteristics of metoprolol during UV/chlorination reaction and a factorial design optimization. *Journal of hazardous materials, 285*, 453-463.

Nika, M.-C., Bletsou, A. A., Koumaki, E., Noutsopoulos, C., Mamais, D., Stasinakis, A. S., & Thomaidis, N. S. (2017). Chlorination of benzothiazoles and benzotriazoles and transformation products identification by LC-HR-MS/MS. *Journal of hazardous materials, 323*, 400-413.

Pillard, D. A., Cornell, J. S., DuFresne, D. L., & Hernandez, M. T. (2001). Toxicity of benzotriazole and benzotriazole derivatives to three aquatic species. *Water research, 35*(2), 557-560.

Reemtsma, T., Miehe, U., Duennbier, U., & Jekel, M. (2010). Polar pollutants in municipal wastewater and the water cycle: occurrence and removal of benzotriazoles. *Water research, 44*(2), 596-604.

Remucal, C., & Manley, D. (2016). Emerging investigators series: the efficacy of chlorine photolysis as an advanced oxidation process for drinking water treatment. *Environmental Science: Water Research & Technology, 2*(4), 565-579.

Ryu, J., Oh, J., Snyder, S. A., & Yoon, Y. (2014). Determination of micropollutants in combined sewer overflows and their removal in a wastewater treatment plant (Seoul, South Korea). *Environmental monitoring and assessment, 186*(5), 3239-3251.

Seeland, A., Oetken, M., Kiss, A., Fries, E., & Oehlmann, J. (2012). Acute and chronic toxicity of benzotriazoles to aquatic organisms. *Environmental Science and Pollution Research, 19*(5), 1781-1790.

Sichel, C., Garcia, C., & Andre, K. (2011). Feasibility studies: UV/chlorine advanced oxidation treatment for the removal of emerging contaminants. *Water research,*

45(19), 6371-6380.

Sun, P., Lee, W.-N., Zhang, R., & Huang, C.-H. (2016). Degradation of DEET and caffeine under UV/chlorine and simulated sunlight/chlorine conditions. *Environmental Science & Technology, 50*(24), 13265-13273.

Trapido, M., Veressinina, Y., & Kallas, J. (2001). Degradation of aqueous nitrophenols by ozone combined with UV-radiation and hydrogen peroxide. *OZONE SCIENCE AND ENGINEERING, 23*(4), 333-342.

Voutsa, D., Hartmann, P., Schaffner, C., & Giger, W. (2006). Benzotriazoles, alkylphenols and bisphenol A in municipal wastewaters and in the Glatt River, Switzerland. *Environmental Science and Pollution Research, 13*(5), 333-341.

Wang, D. (2015). *Application of the UV/Chlorine Advanced Oxidation Process for Drinking Water Treatment.* University of Toronto (Canada),

Weidauer, C., Davis, C., Raeke, J., Seiwert, B., & Reemtsma, T. (2016). Sunlight photolysis of benzotriazoles–Identification of transformation products and pathways. *Chemosphere, 154*, 416-424.

Weiss, S., Jakobs, J., & Reemtsma, T. (2006). Discharge of three benzotriazole corrosion inhibitors with municipal wastewater and improvements by membrane bioreactor treatment and ozonation. *Environmental Science & Technology, 40*(23), 7193-7199.

Weiss, S., & Reemtsma, T. (2005). Determination of benzotriazole corrosion inhibitors from aqueous environmental samples by liquid chromatography-electrospray ionization-tandem mass spectrometry. *Analytical Chemistry, 77*(22), 7415-7420.

Wols, B., Hofman-Caris, C., Harmsen, D., & Beerendonk, E. (2013). Degradation of 40 selected pharmaceuticals by UV/H 2 O 2. *Water research, 47*(15), 5876-5888.

Wu, C., Xu, L., Bian, K., Chen, X., & He, F. (2016). Synergetic degradation of benzotriazole by ultraviolet and ultrasound irradiation. *Desalination and Water Treatment, 57*(38), 17955-17962.

Wu, Z., Fang, J., Xiang, Y., Shang, C., Li, X., Meng, F., & Yang, X. (2016). Roles of reactive chlorine species in trimethoprim degradation in the UV/chlorine process: Kinetics and transformation pathways. *Water research, 104*, 272-282.

Yang, X., Sun, J., Fu, W., Shang, C., Li, Y., Chen, Y., . . . Fang, J. (2016). PPCP degradation by UV/chlorine treatment and its impact on DBP formation potential in real waters. *Water research, 98*, 309-318.

Supplementary material

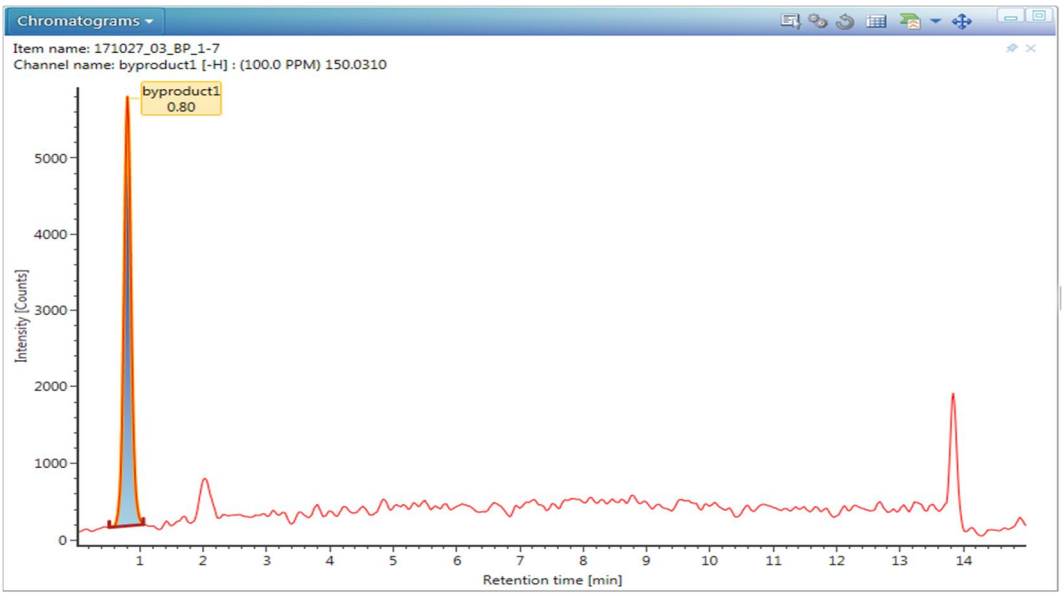

Figure S1. XIC of byproduct 1.

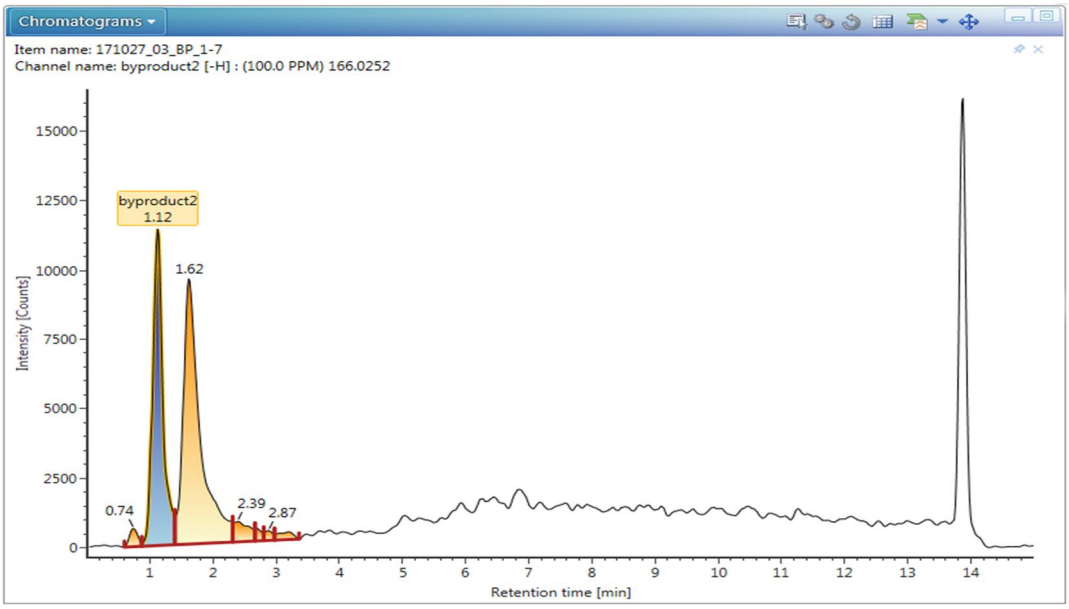

Figure S2. XIC of byproduct 2.

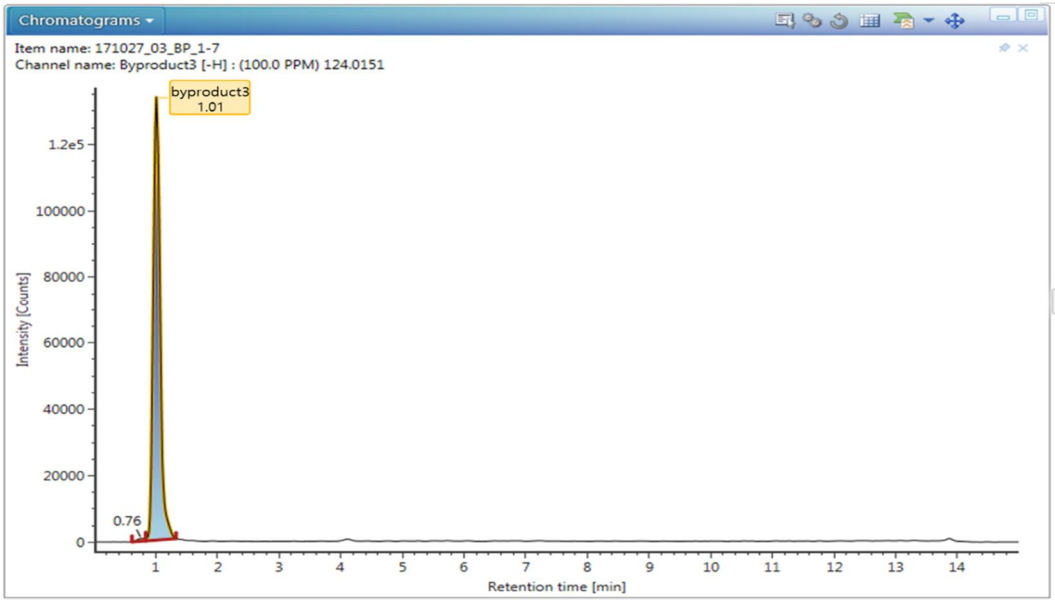

Figure S3. XIC of byproduct 3.

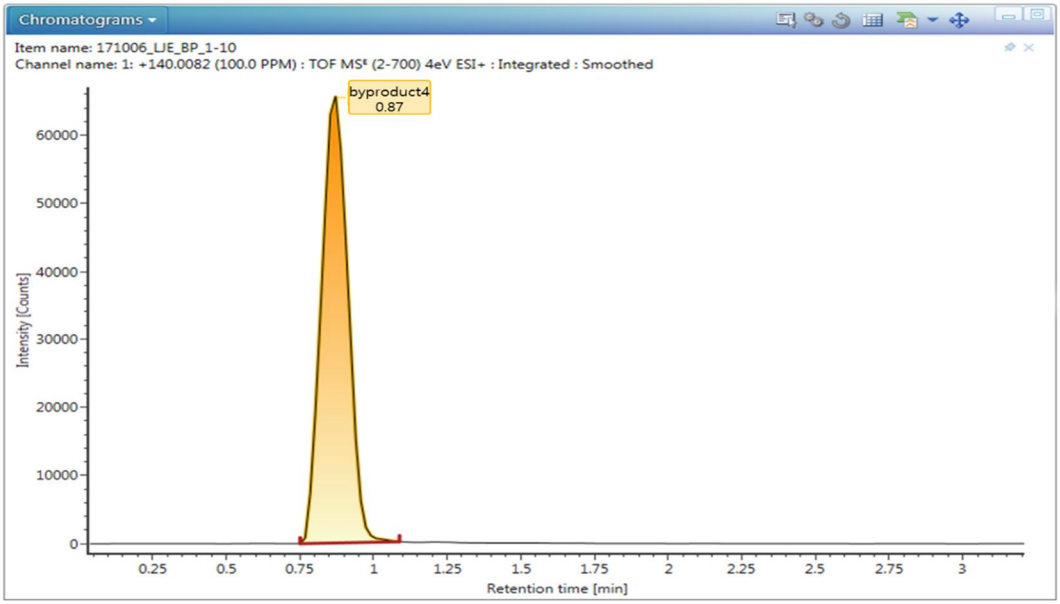

Figure S4. XIC of byproduct 4.

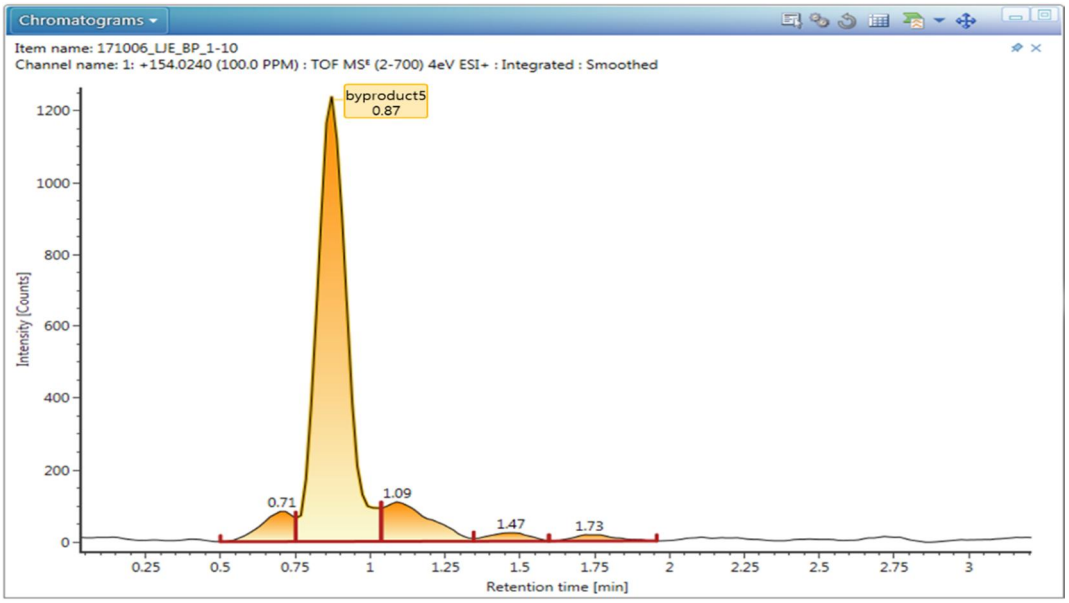

Figure S5. XIC of byproduct 5.

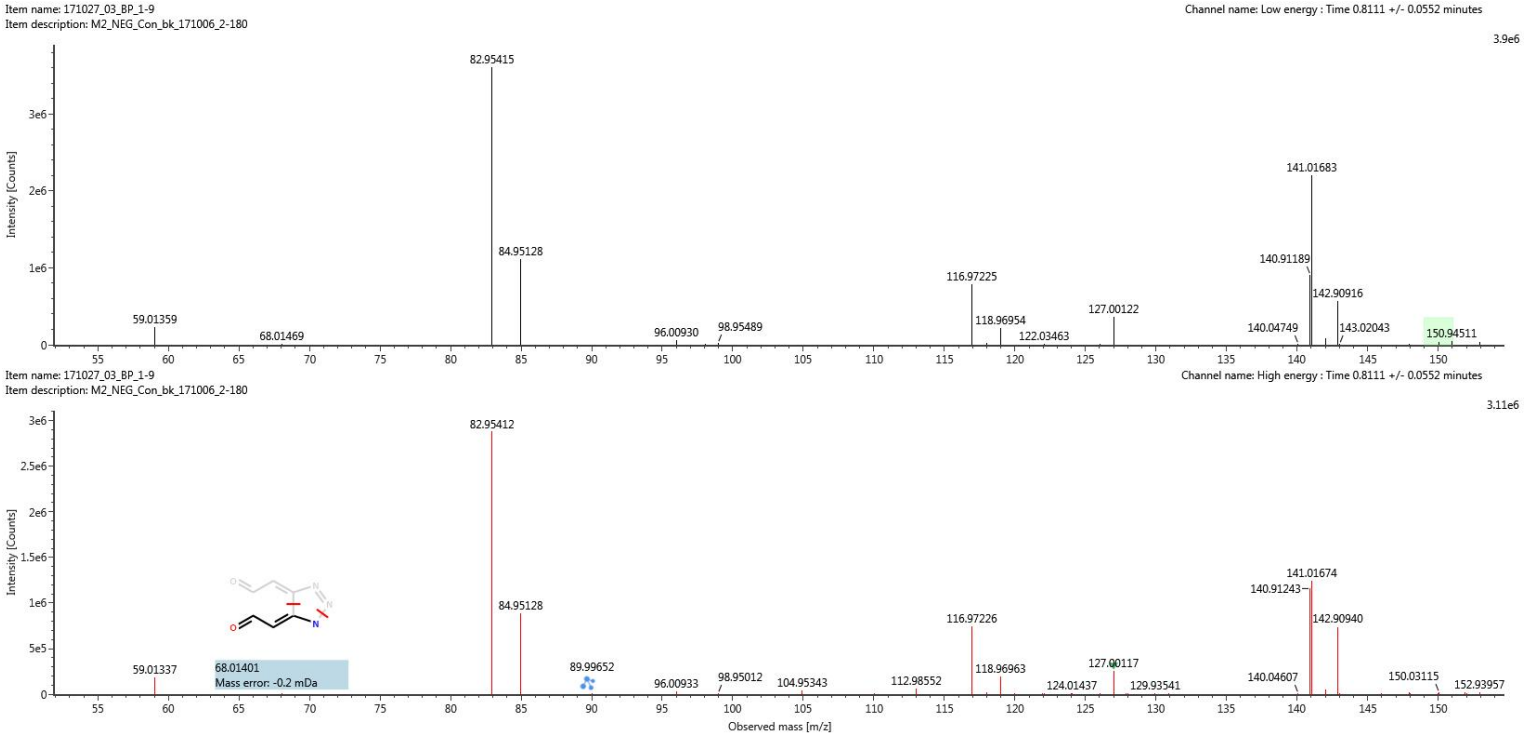

Figure S6. Mass spectra of byproduct 1 (identified by UNIFI).

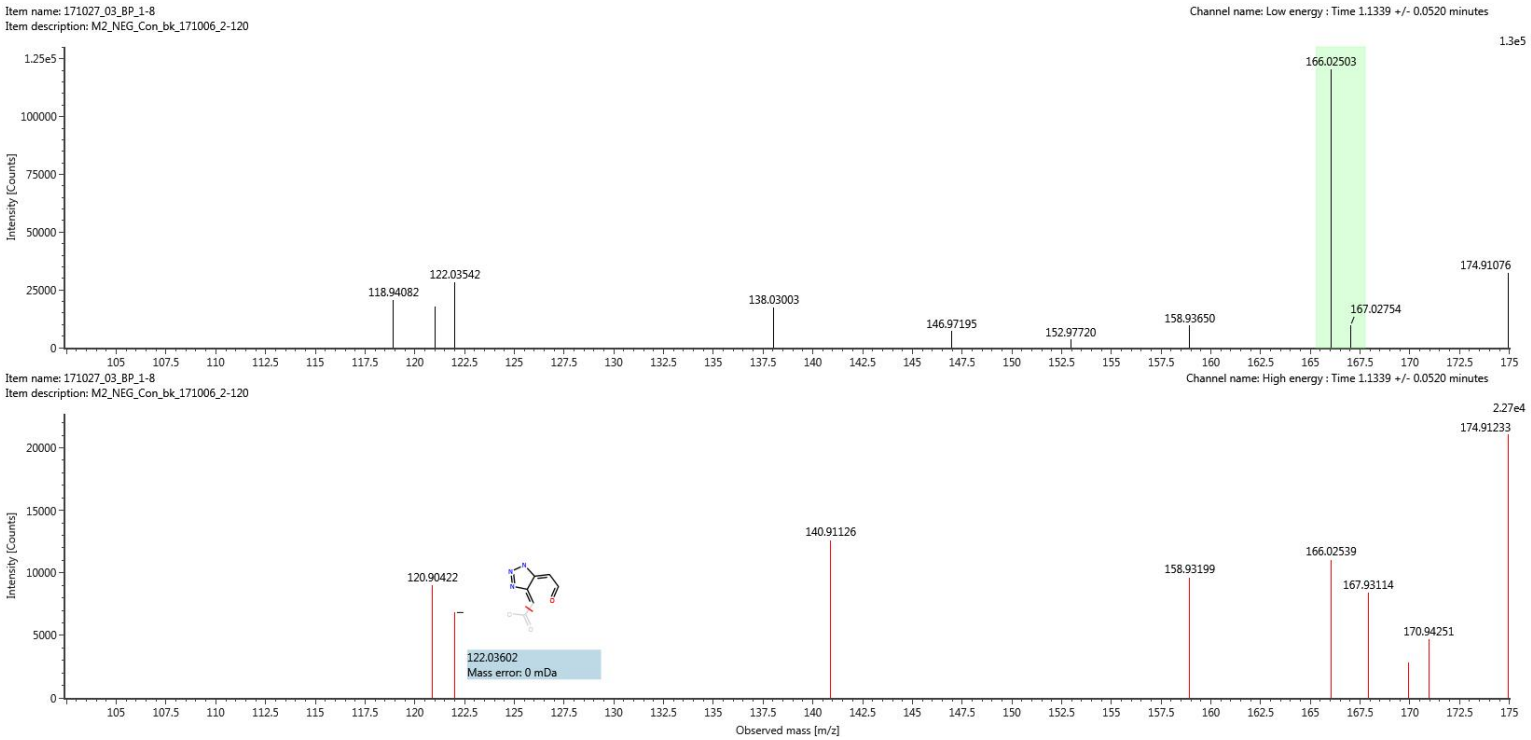

Figure S7. Mass spectra of byproduct 2 (identified by UNIFI).

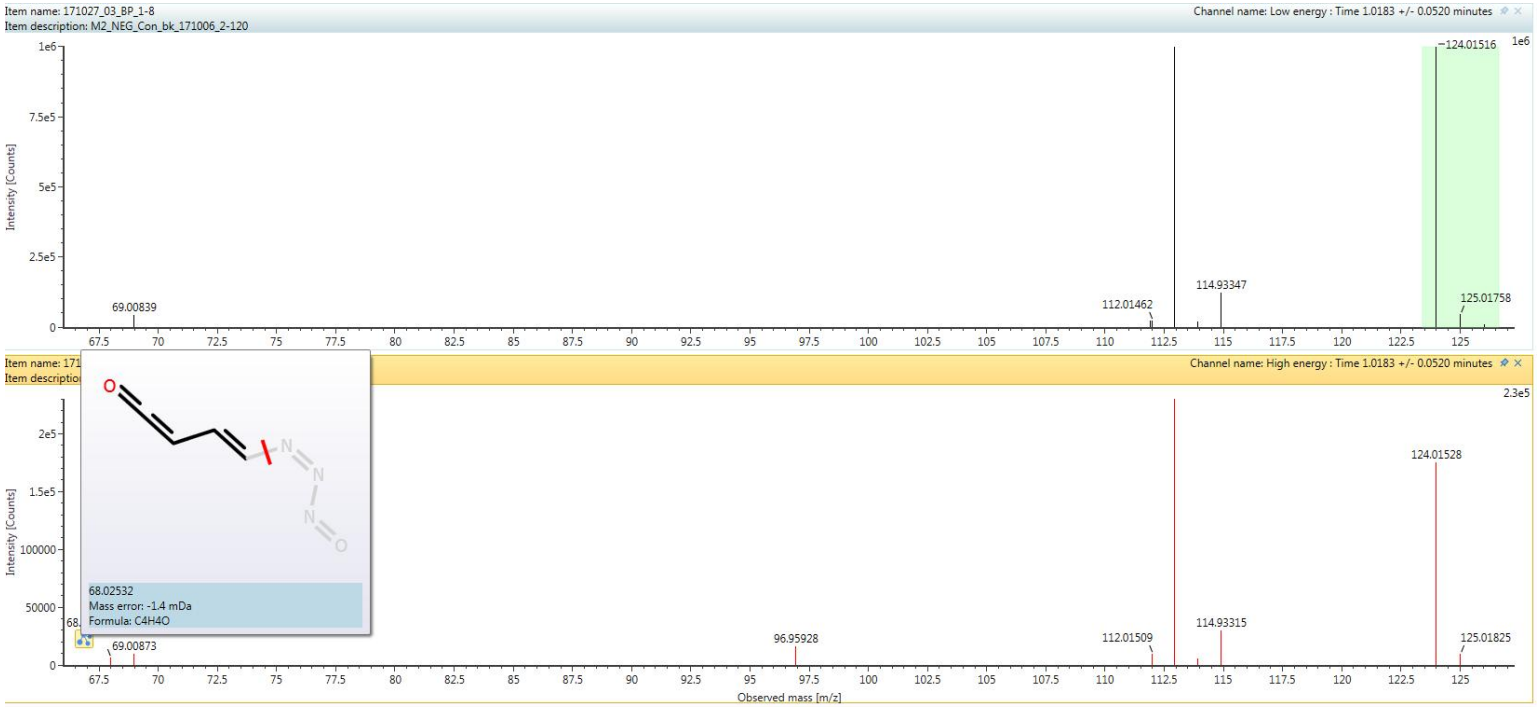

Figure S8. Mass spectra of byproduct 3 (identified by UNIFI).

국문초록

UV/Chlorination 공정 중 1H-benzotriazole의 분해 특성과 메커니즘에 관한 연구

이 정 은

서울대학교 보건대학원

환경보건학과 환경보건학 전공

지도교수 조 경 덕

Benzotriazole (BTA)은 금속과 만나 착물을 형성하여 부식을 방지하는 특성을 가지는 화합물로, 여러 산업에서 금속의 부식방지제, 항공기의 제빙장치, 식기세척기 세제 속의 보호제 등으로 널리 이용된다 (Pillard et al., 2001). 높은 극성과 낮은 생분해성을 가진 이 물질은 기존의 CAS(Conventional Activated Sludge) 공정의 하수처리장에서 부분적으로 제거되는 것으로 알려져 있다 (약

37%의 제거율) (Weiss et al., 2006). BTA는 독일과 중국의 하수처리장 유출수에서 각각 7.7과 2.7 μg/L의 농도로 검출된다고 보고되고 있다 (Weiss et al, 2006; Liu et al, 2013). 이에 따라, 스위스에서는 Benzotriazole을 하수처리장의 'Well eliminated indicator compounds'로 지정하였으며, 최근에는 AOP 공정에 의한 BTA의 제거 특성 연구들이 이루어지고 있다 (Sichel et al., 2011; Borowska et al., 2016). 본 연구에서는 UV 광분해와 염소처리를 결합한 UV/Chlorination 공정을 이용하여 BTA의 분해 특성을 연구하였다.

본 연구를 위하여 특별히 제작된 2L 용량의 batch type reactor를 UV/산화반응 실험에 이용하였으며, 실험에 이용된 UV 램프 (UV-A, UV-B, UV-C)의 세기는 3.3-4.3 mW/cm2이었다. 본 실험에서 BTA는 초기 농도 1 μM (119 μg/L)로, 정해진 반응 시간 마다 50 mL씩 채취 되었으며 총 3시간 동안 반응하였다. Chlorination 및 UV/chlorination을 위한 초기 잔류 염소 농도는 25, 50, 75, 100 μM (1.8, 3.6, 5.3, 7.1 mg/L)이었으며 시료 채취 후 Sodium Thiosulfate 용액을 Chlorination quencher로 이용하였다. quencher 주입을 마친 시료는 1 mL를 바이알에 옮겨 LC-ESI-MS/MS (Shimazu, Japan)로 분석하였다.

본 연구에서는 UV 파장, 잔류 염소 농도, pH의 변화에 따른, BTA의 분해 특성을 알아보았다. 기존 연구에 의하면, BTA는 UV-C 영역에서의 흡광도가 가장 높게 나타났다 (Wu et al., 2016). 이에 따라, UV 파장 별 제거 효율 또한 UV-C 영역에서 가장 높음을 알 수 있다. UV-A와 염소처리의 단일 공정, 조합 공정의 경우, UV-A와 염소의 단일 공정에서는 거의 제거가 되지 않았으나, 두 가지의 조합 공정에서는 염소와 UV의 반응에 의한 OH radical 생성으로 인하여, BTA 제거가 효율적으로 이루어지는 것을 확인할 수 있었다. UV-A/chlorination에 대한 잔류염소 농도 별 제거 속도 실험에서는, 주입하는 유리 염소의 양이 많을수록 생성되는 라디칼의 양이 증가하여 BTA의 제거 반응 속도가 증가하였다. pH의 경우에는, 염기성 > 산성 > 중성의 순서로 반응 속도가 빨랐으며, UV-A 영역의 경우 HOCl 보다는 OCl^-의 흡광도가 상대적으로 높아 OCl^-이 주 종인 염기성에서 가장 빠른 반응 속도를 보이는 것으로 사료된다.

또한, 본 공정 중 BTA의 무기화 정도와 반응부산물, 생태독성의 변화를 알아보았다. 분석 기기의 검출 농도 범위를 고려하여, 기존 실험보다 BTA 및 유리잔류염소의 농도를 100배 높여 실험하였다. BTA는 5시간 안에 모두 제거되었으며, TOC는 5시간 동안 약 40 %, 12시간 동안 약 50 % 제거되어, 50%의 무기화가 일어났음을 확인할 수 있었다. 이에 따라, 50%의 잔류 유기반응 부산물이 있을 것으로 사료되어, 반응부산물을 IC 및 UPLC-qTOF-

MS로 screening 및 identification 하였다. 총 네 가지의 이온부산물 ($HCOO^-$, NO_3^-, ClO_2^-, ClO_3^-)이 검출되었으며, 다섯 가지의 유기 반응 부산물 (m/z 150.0307, 166.0252, 124.0147, 140.0071, 154.0245)이 ESI(positive, negative) 이온화 모드를 이용하여 확인되었다. 본 공정 중 생태독성의 변화는 Microtox test를 통해 측정되었으며, BTA의 UV-A/chlorination 반응 동안 생태독성은 초반에 증가하지만, 반응 종료 시점에는 독성 영향이 현저하게 감소하는 것으로 나타났다.

따라서, 기존 처리공정에서 잘 제거 되지 않아 indicator compounds로 지정되는 물질인 BTA에 대하여, Chlorination과 UV 처리를 조합하여 효과적으로 제거되며, 독성 또한 감소되는 것을 확인할 수 있었다. 이에 따라, 기존 염소처리를 포함한 공정에 UV/chlorination을 적용한다면 난분해성 물질의 제거에 기여할 수 있음을 기대할 수 있다.

주요어: 벤조트리아졸, 난분해성유기물, 고도산화처리, UV-A/chlorination, 분해경로

학번: 2016-24053